Molecular Motions in Polyisobutylene: A Neutron Spin-Echo and Dielectric Investigation

D. Richter,*,† A. Arbe,‡ J. Colmenero,‡ M. Monkenbusch,† B. Farago,§ and R. Faust||

Institut für Festkörperforschung, Forschungszentrum Jülich, 52425 Jülich, Germany, Departamento de Física de Materiales, Universidad del País Vasco, Apartado 1072, 20080 San Sebastián, Spain, Institut Laue-Langevin, 156X, 38042 Grenoble Cedex, France, and Polymer Science Program, Department of Chemistry, University of Massachusetts Lowell, One University Avenue, Lowell, Massachusetts 01854

Received September 11, 1997; Revised Manuscript Received November 26, 1997

ABSTRACT: We present neutron spin−echo and dielectric results on the local dynamics of polyisobutylene. The dielectric spectra reveal the existence of a so far unknown secondary relaxation process being distinctly different to previous theoretical predictions. Neutron spectra have been taken over a large range in momentum transfer Q and temperature. At the Q value of the first structure factor maximum the dynamic pair correlation function is selective for interchain motions. There the neutron spectra display the same temperature dependence and shape as the classical rheological data taken in the terminal zone and do not follow the temperature laws based on spectroscopic results. A quantitative evaluation combining the information content of the dielectric and neutron results reveals a small stepwidth of 0.5−0.9 Å involved in the secondary process. The α process is diffusive and follows the Gaussian approximation resulting in a sublinear time development of associated mean squared displacements.

I. Introduction

The viscoelastic properties of polyisobutylene (PIB) are among those of the most thoroughly investigated properties of any polymer.[1−9] This dates back to an effort by the National Bureau of Standards about 50 years ago, when a large batch of high molecular weight polyisobutylene was distributed to rheological laboratories all over the world. Many of the basic features of polymer rheology have been explored on this material such as the molecular weight dependence of the viscosity, $\eta \propto N^{3.3}$, where N is the degree of polymerization. In his book on viscoelastic properties of polymers[1] Ferry has summed up the rheological data for PIB leading to a temperature-dependent shift factor $a_F(T)$

$$\log [a_F(T)] = -\frac{9.08(T - 298.2)}{209 + T - 298.2} \qquad (1)$$

where T is the absolute temperature. Besides being a focus for the investigation of viscoelasticity, the very stable PIB polymer chain has always been important for commercial exploitation. In particular its unique low permittivity for gases at temperatures well above the glass transition temperature T_g has made it indispensable for the production of tubeless tires.

Although PIB has been the polymer where many viscoelastic particularities of polymer melts have been unraveled, this material exhibits a number of unusual properties which make it stand out among the usual linear chain behavior: (i) PIB appears to be thermorheologically simple—the segmental modes and the terminal relaxation time follow the same temperature-dependent shift factors.[8] (ii) If the temperature-dependent primary relaxation rate of PIB around the glass transition is classified according to the fragility scheme of Angell, then PIB turns out to be the least fragile polymer.[10] In terms of a Vogel Fulcher dependence of the segmental relaxation time, $\tau \propto \exp [DT_\infty/(T - T_\infty)]$, where T_∞ is the Vogel Fulcher temperature, the parameters of eq 1 lead to a fragility index $D = 49$—whereas many other polymers possess D-values in the order of 5. (iii) Going along with the low fragility, the stretching of the mechanical relaxation functions $G(t) = G_0 \exp[-(t/\tau)^\beta]$, where G is the time dependent sheer modulus, is relatively weak. Values for the stretching exponent $\beta \cong 0.5-0.55$ are found[8] which are significantly larger than the more common lower values around $\beta \cong 0.4$ valid for many polymer systems.

Aside of the rheological data, spectroscopic results on the segmental dynamics of PIB with a number of different spectroscopic techniques, like ^{13}C NMR[11,12] or spin label techniques,[6] have been reported. An evaluation of Törmälä[6] shows that in general these spectroscopic methods yield weaker temperature dependencies of the shift factor than the rheological data. This tendency is underlined by recent results from Dejean de la Batie et al.,[12] using the ^{13}C NMR technique. They yield a temperature dependence of the shift factor, which is distinctly weaker than the rheological one.

Though there appears to be no consensus on the existence of a genuine dipole moment within the PIB chain, some dielectric loss experiments on bulk PIB are reported.[13,14] The origin of the dielectric response, thereby, is either related to chain defects due to oxidation or in analogy to the case of propane to a small intrinsic moment of about 0.08 D. The observed position of the main loss peak follows well the temperature dependence of the mechanical data. Some evidence is also brought forward for the existence of a high-frequency secondary β process, though no systematic characterization exists.

The local chain conformation of PIB has been thoroughly investigated by rotational isomeric state (RIS) model approaches,[15] by Monte Carlo computer simula-

† Institut für Festkörperforschung.
‡ Universidad del País Vasco.
§ Institut Laue-Langevin.
|| University of Massachusetts.

S0024-9297(97)01340-5 CCC: $15.00
Published on Web 02/07/1998

tion,[16] and by small angle neutron scattering.[17] The data are consistent with a six-state RIS model, where the main rotational trans and gauche states are split in two substates each. As a consequence of the bulky methyl side groups, the polymer chain locally displays some tendency for a helical conformation.

All the dynamical data presented so far for PIB were obtained either by macroscopic experiments, revealing general temperature dependencies, or by spectroscopic approaches, yielding microscopic time dependencies without length scale information. Here we present a first investigation of the segmental dynamics of PIB on the level of the dynamical pair correlation function as it is measured by neutron spin-echo (NSE) spectroscopy. Studying the dynamic structure factor on the length scales of the inter- and intrachain correlations yields directly space time information on the corresponding motions. In particular, experiments on the first amorphous halo, that means the first structure factor peak, are selective for interchain motions, while experiments at momentum transfers away from the first halo are sensitive to intrachain motion.[18,19]

Though inelastic neutron scattering offers the unique opportunity to resolve atomic or molecular motion in space and time, it generally suffers from a relatively small dynamic range—standard neutron spin-echo experiments, e.g., cover the time range from several pico- to several nanoseconds exploiting, thereby, about 3 decades in time. The interpretation of such measurements can be strengthened considerably if they are combined with a spectroscopic technique providing detailed spectral information over a very broad window in time or frequency. Recently, on the example of polybutadiene (PB), we have demonstrated that such a combination of techniques was essential for a molecular characterization of the secondary relaxation in this material.[18,19]

Thus, to complement the NSE observations, in parallel we also performed dielectric-loss experiments on the same deuterated PIB samples which were exposed to NSE. Though the dielectric response was weak, besides the main relaxation careful measurements unraveled a well-defined high-frequency secondary relaxation. Both temperature dependence and shape information were used as an input for the evaluation of the NSE spectra.

II. Theoretical Considerations on the Dynamic Structure Factor

Neutron spin-echo experiments investigate directly the intermediate dynamic structure factor $S(Q,t)$[20]

$$S(Q,t) = \langle \Delta\rho(Q,t)\Delta\rho(Q,0)\rangle \tag{2}$$

where $\Delta\rho(Q,t)$ is the Fourier component of the density fluctuation corresponding to the wave vector $Q = (4\pi/\lambda)\sin(\theta/2)$ (λ, neutron wavelength; θ, scattering angle) at time t. The pointed brackets denote the thermal average. For $t = 0$, eq 2 describes the usual structure factor $S(Q)$ originating from the short range order in the polymer material.

The dynamic pair correlation function (eq 2) reflects the relative motions of different atom or molecular units with respect to each other. Compared to the self-correlation function which displays the single particle motion, the dynamic pair correlation function is richer in the information content but also much more difficult to calculate. Up to now most of the quasielastic neutron scattering experiments are directed toward the self-motion.[21] Recently, we have presented some considerations on the dynamic pair correlation function due to simple local jump processes and have discussed possibilities for approximations. Furthermore, the dynamic structure factor due to combined local and diffusive type motions was considered.[19]

In this paper we outline the main reasonings, and for a full description we refer to ref 19. Let us first discuss the effect of local jump processes. They underlie for example the β-relaxation or simple conformational jumps. We will describe them in terms of two-site jump processes, where the jump rates are distributed with some distribution function. For the secondary β or Johari Goldstein process[22] in polymers generally log-normal distributions are assumed. Then the individual jump rate $\tau(E)$ is considered to follow an Arrhenius temperature dependence

$$\tau(E) = \tau_0^{\beta} \exp\left(\frac{E}{k_B T}\right) \tag{3a}$$

where the activation energies E are distributed according to a Gaussian distribution function

$$g(E) = \frac{1}{\sqrt{\pi}\sigma} \exp\left\{-\left(\frac{E - E_0}{\sigma}\right)^2\right\} \tag{3b}$$

Thereby σ is the width and E_0 the average activation energy of the distribution, τ_0^{β} a prefactor, and k_B the Boltzmann coefficient. The width $\sigma(T)$ normally depends on temperature.

The isotropically averaged self-correlation function for a two-site jump process can be written down readily

$$S_s(Q,t) = \frac{1}{2}\left[1 + \frac{\sin Qd}{Qd}\right] + \frac{1}{2}\left[1 - \frac{\sin Qd}{Qd}\right] \exp\left[-\frac{2t}{\tau(E)}\right]$$

$$S_s(Q,t) = S_{el} + S_{inel} \exp\left[-\frac{2t}{\tau(E)}\right] \tag{4}$$

where d is the distance between the two sites. The pair correlation function differs from the self-correlation function by the presence of interference effects of the waves scattered from the initial and final configuration of atoms. For the static scattering ($t = 0$ in eq 2) these interference effects give rise to the static structure factor $S(Q)$. The simplest approximation we can make is to assume that the jumping atoms are uncorrelated. Then all interference effects from the moving atoms drop out and the inelastic contribution to the dynamic pair correlation function can be approximated by that of the self-correlation function (eq 4, second part). This approximation immediately leads to

$$\frac{S(Q,t)}{S(Q)} = \frac{S(Q) - S_{inel}(Q)}{S(Q)} + \frac{S_{inel}(Q)}{S(Q)} \exp\left[-\frac{2t}{\tau(E)}\right] \tag{5}$$

To arrive at the appropriate structure factor for the local β-relaxation, eq 5 has to be averaged over the distribution functions (eq 3). The consequence of the incoherent approximation is a renormalization of the relative inelastic self-contribution of local jumps by the static structure factor $S(Q)$—in Q regimes where the static structure factor is strongly peaked, in particular at the first peak of S(Q), contributions from the local dynamics are strongly suppressed, while they are visible

in particular in the regions of the structure factor minima. This diminution of the inelastic contributions to $S(Q,t)$ in the peak regions of $S(Q)$ resembles the so-called de Gennes' narrowing for diffusive processes.[23] There, a modulation of the Q-dispersion of the relaxation rate $\Gamma(Q) \sim DQ^2$, where D is the diffusion coefficient, with $1/S(Q)$ takes place. For a local two-site jump process the relaxation rate does not exhibit dispersion in Q and the apparent de Gennes' narrowing translates into a modulation of the relative weight factors for the inelastic contributions to $S(Q,t)$ with $1/S(Q)$.

In our description of the dynamics of PB we have shown that the assumption of statistically independent diffusive α and local β processes leads to a consistent description of the dynamical data. For statistically independent processes taking place simultaneously the combined self-correlation function results from a convolution product of the corresponding self-correlation functions in real space. In Fourier space this implies that the combined dynamic structure factor $S_S^{\alpha\beta}$ can be written as a direct product of the structure factors of the α [$S_S^{\alpha}(Q,t)$] and β relaxation [$S_S^{\beta}(Q,t)$]

$$S_S^{\alpha\beta}(Q,t) = S_S^{\alpha}(Q,t)S_S^{\beta}(Q,t) \tag{6}$$

Unfortunately, this simple relationship cannot be easily taken over for the pair correlation function. In ref 19 we have shown that applying a Vineyard approximation to the α process $S^{\alpha\beta}(Q,t)$ can be expressed as

$$S^{\alpha\beta}(Q,t) = \varphi^{\alpha}(Q,t)\, S^{\beta}(Q,t) \tag{7}$$

where $S^{\beta}(Q,t)$ is the dynamic structure factor of the β relaxation and $\varphi^{\alpha}(Q,t)$ is the incoherent approximation for the correlation function of the α process

$$\varphi^{\alpha}(Q,t) = \exp\left\{-\left(\frac{t}{\tau_{\mathrm{KWW}}(Q,T)}\right)^{\beta}\right\} \tag{8}$$

For the correlation function of the α-relaxation we take the stretched exponential (KWW) form with the stretching exponent β and a T- and Q-dependent correlation time $\tau_{\mathrm{KWW}}(Q,T)$.

We summarize the main results on the dynamic structure factor: (i) The dynamic pair correlation function for local jump processes may be obtained from the corresponding self-correlation function in introducing a "de Gennes' narrowing" for the relative weights for the inelastic contributions. (ii) Considering the α relaxation as simultaneous and statistically independent from the β relaxation, the corresponding dynamic structure factors are multiplicative. (iii) Due to the "de Gennes' narrowing" of the inelastic weight factors for the local processes, at the first structure factor maximum $S(Q,t)$ is dominated by the α relaxation. Thus, there exists a "Q-selectivity" allowing an observation of the diffusive α relaxation basically unperturbed by local relaxation processes.

III. Experimental Section

III.1. Sample Preparation and Characterization. Materials and procedures. Sources and purification of materials have been described.[24] Living cationic polymerization of deuteroisobutylene (99% chemical purity, CDN Isotopes) was carried out in a 500 mL three-neck flask equipped with an overhead stirrer at −80 °C under a dry ([H_2O] < 1.0 ppm) nitrogen atmosphere in an MBraun 150-M glovebox. The target number average molecular weight (M_n) of deuteropolyisobutylene was 70 000. A 8.7 mL portion of a hexane (Hex) stock solution (0.2406 g/25 mL) of the initiator, 5-*tert*-butyl-1,3-bis-(1-chloro-1-methylethyl)benzene (tBuDiCumCl), 0.263 mL of 2,6-di-*tert*-butylpyridine (DTBP), as a proton trap, and 171 mL of Hex were charged to the flask at room temperature. The temperature was lowered to −80 °C and 94 mL of methyl chloride (MeCl) was added to reach the final ratio of Hex/MeCl = 60/40 (v/v) at −80 °C. Then 12.9 mL of $TiCl_4$ stock solution in MeCl (7 mL of $TiCl_4$ in 50 mL) was added. Deuteroisobutylene was introduced to the flask in three equal increments 8.3 mL each, in 15 min intervals. The polymerization was quenched with prechilled methanol. After evaporation of the volatiles, 20.4 g of deuteropolyisobutylene (monomer conversion = 100%) was obtained. Purification procedure of the product has already been reported.[24]

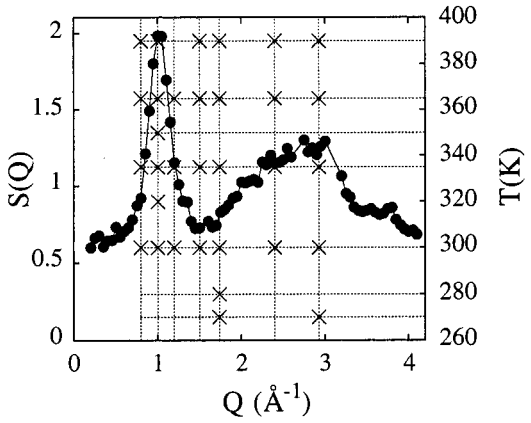

Figure 1. Static structure factor of polyisobutylene at room temperature (●). Crosses indicate the positions in (Q,T) space where the NSE experiments were performed.

Characterization. The molecular weight of deuteropolyisobutylene (M_n = 72 000) and polydispersity (M_w/M_n = 1.05) were measured using a Waters high-performance liquid chromatography (HPLC) system equipped with a Model 510 HPLC pump, Model 410 differential refractometer, Model 486 tunable UV/Vis detector, on-line multiangle laser light scattering (MALLS) detector (miniDawn, Wyatt Technology Inc.), Model 712 sample processor, and five Ultrastyragel gel permeation chromatography (GPC) columns connected in the following series: 500, 10^3, 10^4, 10^5, and 100 Å. The flow rate of tetrahydrofuran eluent was 1.0 mL/min.

III.2. Dielectric Experiments. The dielectric response $\epsilon^*(\omega) = \epsilon'(\omega) + i\epsilon''(\omega)$ of PIB was investigated in the frequency range 10^{-1} to 10^6 Hz by using a frequency response analyzer Schlumberger SI 1260 equipped with a Chelsey dielectric interface with high impedance preamplifier. The sample holder consisted of a parallel-plate capacitor (diameter 20 mm), where the distance between the plates (0.1 mm) was kept constant by insertion of small Teflon spacers.[25]

Under isothermal conditions (temperature stability better than 0.1 K) the real and imaginary parts of the dielectric permittivity were measured in the temperature range 120 K = T = 200 K each 5 K and in the region 200 K = T = 300 K each 2.5 K.

The measuring time was about 10 times longer than the standard time for typical polymers due to the small dipole moment of PIB.

III.3. NSE Experiments. The static structure factor $S(Q)$ was obtained from the fully deuterated PIB-sample using the triple axis spectrometer SV4 at the FRJ-2 research reactor in Jülich, Germany. Thereby the instrument was used in a two-axis mode with pyrolytic graphite as a monochromator (incoming neutron wave vector k_i = 2.54 Å^{-1}). Figure 1 displays the background-corrected data taken at room temperature. $S(Q)$ is characterized by a first strong peak at Q = 1 Å^{-1} and a broad second peak in the Q regime 1.7 ≤ Q ≤ 3.4 Å^{-1}. The first peak or amorphous halo shifts strongly with temperature and results mainly from interchain correlations. Its position at Q_{max} = 1 Å^{-1} indicates a relatively large distance between

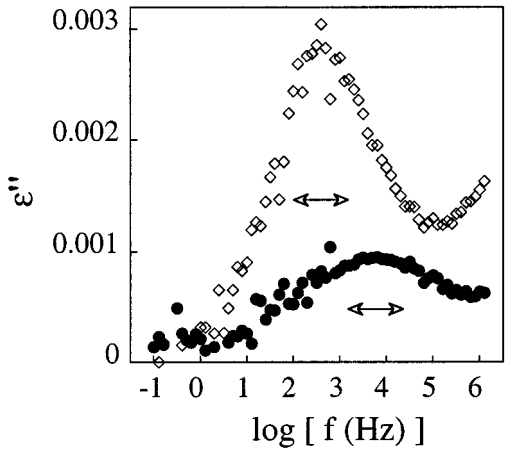

Figure 2. Frequency dependence of the dielectric loss spectra of PIB at 160 K (●) and 230 K (◇). The arrows show the fwhm corresponding to Debye processes for comparison.

neighboring chains of $d = 2\pi/Q_{max} \approx 6.3$ Å, considerably larger than for other typical main chain polymers. The second broad peak at higher Q is temperature insensitive and relates to a large extent to intrachain correlations.

The neutron spin-echo experiments were performed by means of the spectrometer IN11 at the Institute Laue-Langevin (ILL) in Grenoble, France, and using the new Jülich NSE spectrometer.[26] As described elsewhere,[20] NSE measures directly the normalized intermediate scattering function $S(Q,t)$ (eq 2). Since due to the spin flip scattering, the incoherent scattering contributions are strongly suppressed; the signal from the deuterated PIB sample is nearly entirely due to coherent scattering revealing the pair correlation function.

Figure 1 displays an overview over the experimental program undertaken, each cross stands for a (Q,T) point measured. To span the Q range 0.8 Å$^{-1} \le Q \le$ 2.93 Å^{-1}, different neutron wavelengths λ and different scattering angles had to be employed. Since the maximum Fourier time relates to the third power of the neutron wavelength, different wavelengths imply different time ranges which are covered. At IN11 the following Q and time ranges were explored: $Q = 1.0$ Å^{-1} ($\lambda =$ 5.1 Å), 5 ps $\le t \le$ 3 ns; $Q = 1.5$ Å^{-1} ($\lambda = 4.7$ Å), 3 ps $\le t \le$ 3 ns; $Q = 1.74$ Å^{-1} ($\lambda = 5.1$ Å), 5 ps $\le t \le$ 3 ns; $Q = 2.4$ Å^{-1} ($\lambda =$ 4.7 Å, 3 ps $\le t \le$ 3 ns; $Q = 2.93$ Å^{-1} ($\lambda = 3.85$ Å), 2 ps $\le t \le$ 1.3 ns. At the Jülich machine, experiments were performed at $\lambda = 8$ Å accessing the Q value $Q = 0.8$ Å^{-1} and at $\lambda = 7$ Å reaching $Q = 1.2$ Å^{-1}. In each case the time window was 0.1 $\le t \le$ 16 ns.

For each momentum transfer, the instrumental resolution function was measured from the elastic scattering of the sample at 4 K. The instrumental background from the cryostat and from the Al container were measured separately and subtracted from the experimental spectra using the appropriate transmission factors. Thereby the most important background was found at the highest Q value, where the multiple Bragg scattering from the aluminum resulted in an elastic background of about 20% of the total signal. In Jülich a sample container made from an Aluminum single crystal was used which reduced the background from the sample environment significantly. The background-corrected spectra were divided by the resolution function in order to obtain the normalized intermediate dynamic structure factors $S(Q,t)/S(Q)$.

IV. Experimental Results

IV.1. Dielectric Results. As can be seen in Figure 2, at temperatures below T_g only one relaxational process, the β relaxation, is active in our experimental window. With increasing temperature the maximum of the loss peak corresponding to this process shifts toward high frequencies. Above T_g and at lower frequencies than the characteristic frequency of the secondary process, the α relaxation contribution to the dielectric response can also be observed. Figure 2 shows as an example $\epsilon''(\omega)$ at $T_g + 30$ K, where the loss peak of the α relaxation is approximately centered in our experimental window and the β-loss peak sets in at about 10^5 Hz. While at this temperature both loss processes are well separated, they approach each other with increasing temperature. This is evidenced in Figure 3, where the temperature dependence of the characteristic frequency for both relaxations is shown in comparison with the relaxation map proposed by Törmälä in ref 6 for PIB. As can be seen from this figure, our results for the α relaxation agree well with those shown in the compilation of spectroscopic data by Törmälä. However, the characteristic frequencies of the β-relaxation obtained by us cannot be related to any of the secondary relaxations proposed in that compilation. The disagreement with the two processes denoted as γ and γ', which were theoretically predicted by Stoll et al.,[14] is evident. Moreover, although the temperature dependence of the dielectric β process is similar to that observed for the so-called δ process, which is interpreted as rotations of $-CH_3$ groups, the dielectric process takes place at ≈1.5 orders lower frequencies. Furthermore, methyl group rotation is not dielectrically active.

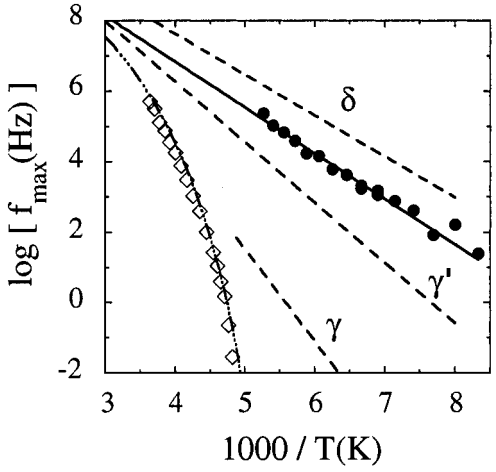

Figure 3. Arrhenius plot of the characteristic frequencies (corresponding to the maximum of the dielectric loss) of the α (◇) and β relaxation (●). The solid line represents a fit with an Arrhenius law. Dashed−dotted and dashed lines are the temperature laws shown in ref 6 for the α relaxation and the different secondary relaxations, respectively.

To obtain a more quantitative description of the β process, we can analyze the dielectric spectra by assuming that α and β relaxations are statistically independent processes. At temperatures well below their coalescence, this approach reduces to a simple addition of their contributions for the description of the total dielectric function,[19,27] i.e., $\epsilon^*(\omega) - \epsilon_\infty = \Delta\epsilon_\alpha\, \Phi_\alpha^*(\omega) + \Delta\epsilon_\beta\, \Phi_\beta^*(\omega)$, where ϵ_∞ is the infinitive frequency limit of the real part of the dielectric function and $\Delta\epsilon_\alpha$ ($\Delta\epsilon_\beta$) and $\Phi_\alpha^*(\omega)$ [$\Phi_\beta^*(\omega)$] are the relaxation strength and the response function of the α relaxation (β relaxation), respectively. The response functions of both relaxations are clearly different from a Debye process, $\Phi_D^*(\omega) = (1 + i\omega\tau)^{-1}$, which is characterized by a full width at half-maximum (fwhm) of ∼1.14 decades in frequency (see Figure 2). We can consider the stretching of the response functions as due to distributions of Debye processes in the sample. As already mentioned in section II, in the case of the secondary relaxation a distribution function of relaxation times $g_\beta(\ln \tau)$ reflect-

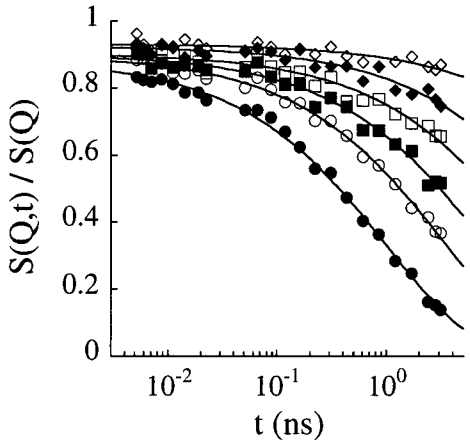

Figure 4. NSE spectra obtained by IN11 at $Q_{max} = 1.0$ Å^{-1} and different temperatures: 300 K (◇); 320 K (◆); 335 K (□); 350 K (■); 365 K (○) and 390 K (●). Solid lines are the fit results corresponding to KWW laws with $\beta = 0.55$.

ing a Gaussian distribution of energy barriers $g(E)$ (eq 3b) in the material is usually considered. Taking into account eqs 3a and 3b we obtain

$$g_\beta(ln\ \tau) = \frac{k_B T}{\sqrt{\pi\sigma}} \exp\left\{-\left(\frac{k_B T \ln(\tau/\tau_0{}^\beta) - E_0}{\sigma}\right)^2\right\} \quad (9)$$

and the response function of the β relaxation is given by

$$\Phi_\beta{}^*(\omega) = \int_{-\infty}^{+\infty} g_\beta(\ln\ \tau)\, \frac{1}{1 + i\omega\tau}\, \mathrm{d}(\ln\ \tau) \quad (10)$$

For the contribution of the α relaxation we assume a KWW-like functional form (eq 8) for its relaxation function in the time domain. In this work we are mainly interested in the description of the secondary relaxation and therefore we will not go into further detail concerning the dielectric results for the α process.

A description of the dielectric data in terms of eqs 9 and 10 results in the following values for the parameters characterizing the time scale of the β relaxation: $\tau_0{}^\beta = 1.5 \times 10^{-13}$ s and $E_0 = 0.26$ eV. The temperature dependence for the distribution width σ can approximately be described by a linear regression

$$\sigma(\mathrm{eV}) = 0.13 - 2.9 \times 10^{-4}\, T\ (\mathrm{K}) \quad (11)$$

IV.2. NSE Results. Figure 4 displays experimental spectra obtained at the first peak of the static structure factor $S(Q)$ at $Q_{max} = 1$ Å^{-1} for the temperature range $300 \le T \le 390$ K. All data sets cover 3 decades in Fourier time. This large time range was achieved by a double spin−echo setup where for the short times a small main coil was used as the precession coil.[28] The data were fitted with a KWW function (eq 8) and are well described by a stretching exponent of $\beta = 0.55$. We note that the amplitudes of the dynamic structure factor $S(Q,t)/S(Q)$ decrease slightly with increasing temperature. While this effect is minute at Q_{max}, it will become significant at higher Q values (see below).

To perform time−temperature superposition these changing amplitudes have to be considered. Thereby we have applied the following procedure: The spectra at a given Q value measured at different temperatures were fitted with a stretched exponential allowing for a different amplitude for each temperature but keeping a common stretching parameter β. In all cases the logarithms of the such obtained temperature-dependent spectral amplitudes $A(Q,t)$ could be well described by a linear regression yielding interpolated amplitudes $\hat{A}(Q,t)$ (see, e.g., insert in Figure 8). In a second step the observed spectral amplitudes were renormalized to the value at 300 K by multiplying the respective spectra with $\hat{A}(Q,300\ \mathrm{K})/\hat{A}(Q,t)$.

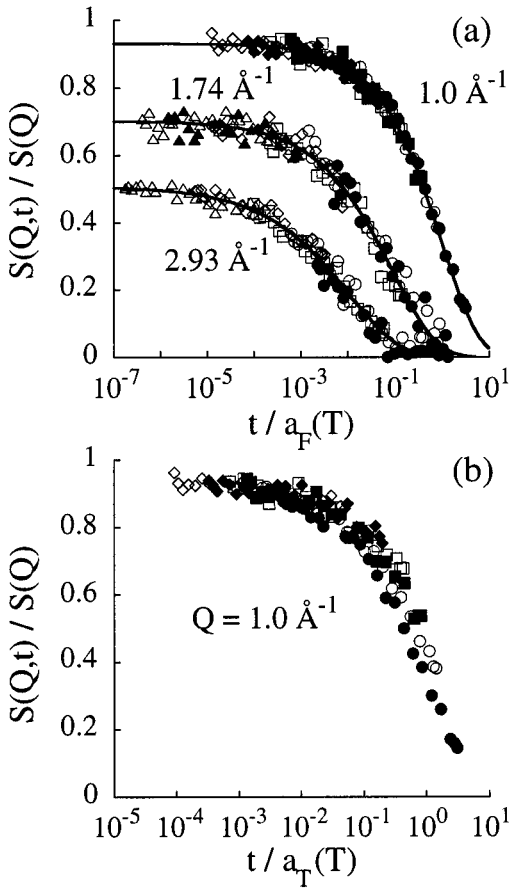

Figure 5. Scaling representation of the NSE spectra at Q_{max} using the shift factors given by Ferry[1] (a) and Törmälä[6] (b). The reference temperature is 390 K. Part a also includes master curves obtained by shifting spectra at $Q = 1.74$ Å^{-1} and 2.93 Å^{-1} with the shift factors of Ferry. Symbols correspond to different temperatures: 270 K (△); 280 K (▲); 300 K (◇); 320 K (◆); 335 K (□); 350 K (■); 365 K (○) and 390 K (◆). Solid lines are fits to KWW functions.

Time-temperature shifts of the such renormalized spectra are now employed in order to assess the temperature dependence of the NSE spectra in comparison to that of the rheological or spectroscopic data. For that purpose the NSE spectra were shifted (i) with a rheological shift factor, we take that due to Ferry (eq 1), and (ii) with a typical spectroscopic shift factor as evaluated by Törmälä $a_T(T)$ [log $[a_T(T)] = -11.0\ (T - 211)/(T - 155)$]. The results of this procedure are presented in Figure 5. While the rheological shift factor leads to a collapse of all spectra on a single master curve which can be well described by a stretched exponential with $\beta = 0.55$, the spectroscopic shift factor does not assemble the spectra to form a master curve. Obviously, the dynamic pair correlation function at the position of the first peak of the static structure factor displays the same temperature dependence and even the same stretching as the mechanical relaxation measured in the terminal regime of the dynamic modulus.

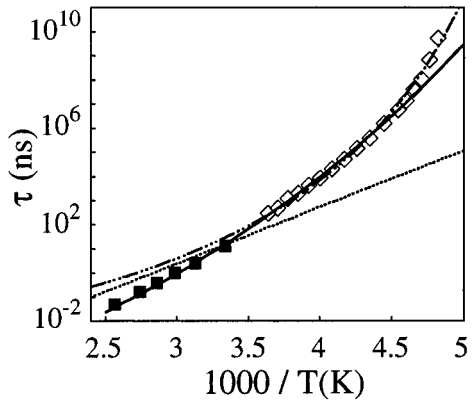

Figure 6. Temperature dependence of the characteristic time of the α relaxation as measured by dielectric spectroscopy (defined as $(2\pi f_{max})^{-1}$) (◇) and of the shift factor obtained from the NSE spectra at $Q_{max} = 1.0$ Å^{-1} (■). The different lines show the temperature laws proposed by Törmälä[6] from spectroscopic data (dashed−dotted), by Ferry[1] from compliance data (solid), and by Dejean de la Batie[12] from NMR data (dotted).

At the Q value of the first structure factor peak Q_{max} the pair correlation function is dominated by the relative motion of adjacent chains. The observation that both mechanical relaxation as well as the pair correlation function at Q_{max} are described by the same temperature and time dependent relaxation function strongly indicates that the temperature dependence of the mechanical relaxation relates to the relative chain motion on the level of adjacent chains. On the other hand the discrepancies with the temperature law based on the spectroscopic data which in principle are also sensitive to microscopic motions show that those spectroscopic data, in particular NMR, are not selective for specific dynamics such as the pair correlation function but subsume all local motions including segmental relaxations. This apparently leads to a weaker temperature dependence.

Figure 6 compares quantitatively the temperature dependencies of the α relaxation times τ_{KWW} obtained from fitting the individual NSE spectra by eq 8 with the compliance data of Ferry,[1] the ^{13}C NMR results of Dejean de la Batie,[12] and the compilation of data by Törmälä.[6] Again as appeared already from Figure 5, the discrepancies between the NSE results and the spectroscopic temperature law (dashed−dotted line[6] and dotted line[12]) become obvious, while the good agreement with the rheological data is documented also in the comparison with the single shift factors.

Now we will inspect NSE spectra at momentum transfers away from Q_{max}. Figure 7 displays spectra at $Q = 0.8$ Å^{-1}, at the lower Q flank of the structure factor maximum. These data were taken at the NSE spectrometer in Jülich. The data are again fitted by a stretched exponential yielding $\beta = 0.48$. The shift factors are indistinguishable from the rheological shift factor given by Ferry.

As another example Figure 8 displays some experimental spectra taken at $Q = 2.93$ Å^{-1}, the largest momentum transfer which could be reached. Three observations are noteworthy: (i) At short times the spectra commence with a significantly lower amplitude than those taken at lower Q. The fast dynamic processes, present in glass forming polymers,[29,30] lead to a large apparent Debye−Waller factor which reduces the amplitude of the spin-echo signal significantly at high Q. These processes occur at times shorter than the shortest spin−echo time of about 2 ps but within the band-pass of the instrument. Therefore they contribute to the normalization of $S(Q,t)$ by $S(Q)$ but are not visible directly in the NSE time window. The insert in Figure 8 displays the temperature-dependent spectral amplitude $A(Q,t)$ which shows the above-mentioned linear regression from $A \approx 0.6$ at 270 K to $A \approx 0.4$ at 390 K. (ii) Compared to the spectra at lower Q, in the high Q region the relaxation spectra decay at much shorter times. For 390 K the essential spectral decay occurs between 10 and 100 ps, nearly 2 orders of magnitude faster than that at $Q = 1$ Å^{-1}. (iii) Finally, the relaxation spectra are significantly more stretched than in the low Q region yielding a β value of $\beta = 0.4$.

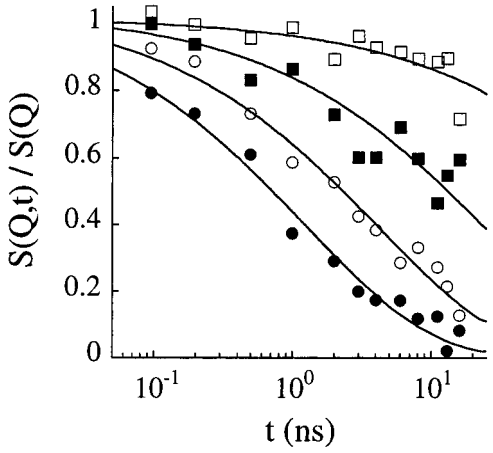

Figure 7. Spectra obtained by the NSE spectrometer in Jülich at $Q = 0.8$ Å^{-1} and at 300 K (□), 335 K (■), 365 K (○), and 390 K (●). Solid lines are the fit results corresponding to KWW laws with $\beta = 0.48$.

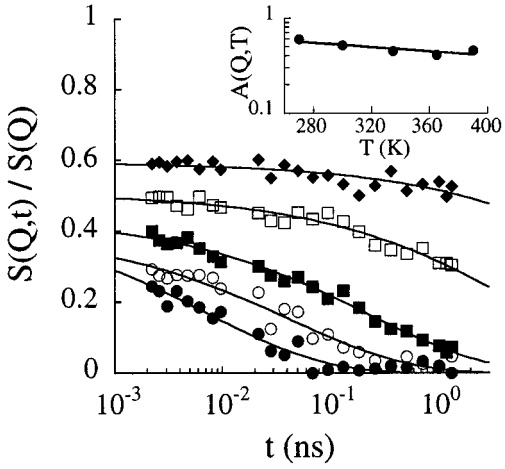

Figure 8. NSE spectra obtained by IN11 at $Q = 2.93$ Å^{-1} and at 270 K (◆), 300 K (□), 335 K (■), 365 K (○), and 390 K (●). Solid lines are the fit results corresponding to KWW laws with $\beta = 0.40$. The insert shows the temperature dependence of the prefactors $A(Q,T)$ at this Q value. The solid line represents the result of a linear regression.

Figure 5a displays the same spectra in a scaling representation. The data were renormalized to the amplitude at 300 K (see above) and shifted with the rheological shift factor $a_F(T)$ of Ferry. Again within experimental accuracy these data do not significantly deviate from the rheological temperature scale. However, in particular due to the small spectral amplitude the accuracy of the spectral data is reduced compared to that at Q_{max}.

Table 1. Parameters from Fitting the Master Curves Which Were Assembled in Scaling the NSE Spectra at the Different *Q* Values with the Shift Factors of Ferry (eq 1): Characteristic Time τ_{KWW}, Shape Parameter β, Average Relaxation Time $\langle\tau\rangle = \Gamma(1/\beta)\,\tau_{KWW}/\beta$, and Amplitude Factors at 300 K[a]

Q (Å^{-1})	τ_{KWW} (ns)	β	$\langle\tau\rangle$ (ns)	A (Q,300 K)
0.8	1.4	0.48	3.0	1.02
1.0	0.98	0.55	1.67	0.93
1.2	0.31	0.56	0.51	1.00
1.5	0.15	0.55	0.26	0.68
1.74	0.086	0.46	0.20	0.70
2.4	0.052	0.40	0.17	0.74
2.93	0.010	0.40	0.033	0.51

[a] The reference temperature for the time scale is 390 K.

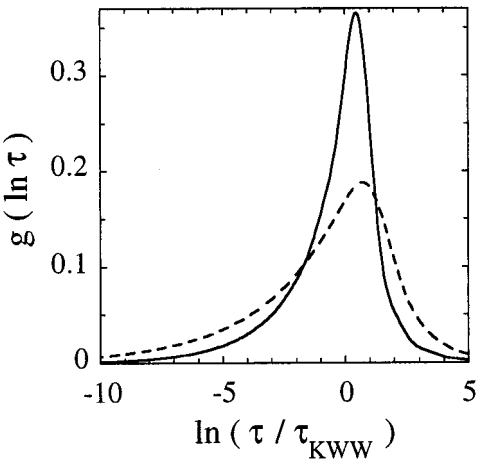

Figure 9. Distribution functions of relaxation times corresponding to KWW functions with $\beta = 0.55$ (solid line) and $\beta = 0.40$ (dashed line).

With similar success also all other spectra (see, e.g., $Q = 1.74$ Å^{-1} in Figure 5a) can be shifted with the rheological shift factor $a_F(T)$ yielding experimentally acceptable single master curves. Depending on Q, however, the relaxation times and the β values change. Table 1 displays the parameters obtained from a fit of the shifted relaxation spectra at different momentum transfers. The reference temperature was always 390 K. For different Q these stretching parameters vary from $\beta = 0.58$ at $Q = 1.2$ Å^{-1} to $\beta = 0.4$ at $Q = 2.9$ Å^{-1}. At the same time the relaxation times at $T = 390$ K are spread from 1.4 ns at $Q = 0.8$ Å^{-1} to 0.01 ns at $Q = 2.93$ Å^{-1}.

Stretched exponential relaxation functions can be interpreted and represented by distributions of relaxation times $g(\ln\tau)$. Figure 9 displays schematically such distributions for $\beta = 0.55$—the α process—and for $\beta = 0.4$ ($Q = 2.9$ Å^{-1}). The different curves in Figure 9 depict the essential of the observed different stretching exponents. At high Q the NSE spectra decay in a broader time range indicating the presence of extra relaxation processes not existing within the α process. Thus, though for all momentum transfers the average relaxation time appears to shift with the Ferry shift factor $a_F(T)$, the different stretching parameters β observed at different Q evidence the presence of further relaxation processes which become visible outside the first structure factor peak.

V. Interpretation and Discussion

Up to now a similar microscopic investigation of the dynamic structure factor from a glass-forming polymer has only been reported for polybutadiene (PB).[18,19] This material has been thoroughly investigated covering a similar range in momentum transfer and Fourier time. As for PIB the interchain relaxation in PB measured at Q_{max} maps to the viscosity temperature scale. Similar to PIB also for PB at Q values different to Q_{max} broader relaxation spectra have been found. On the other hand in the case of PB at the first and second structure factor peak significantly and qualitatively different temperature dependencies were observed. While for PIB within experimental accuracy all data at all momentum transfers can be described by the same temperature shift factors following from rheology, in PB the high Q data scale perfectly with the Arrhenius-like temperature dependence of the dielectric β relaxation.

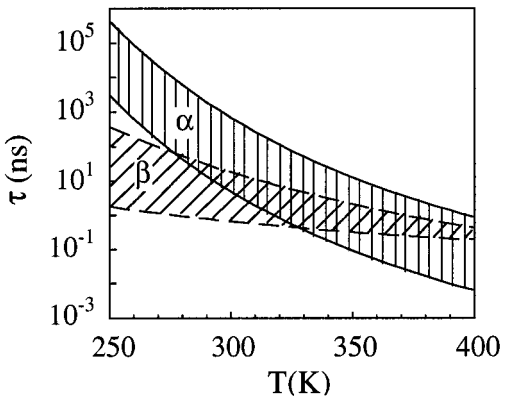

Figure 10. Temperature dependence of the relaxation times for the α and β relaxations: the $\tau_{KWW}(Q,t)$ for the different Q values investigated lay in the dashed area between the solid lines (the upper one represents $\tau_{KWW}(Q = 0.8$ Å^{-1}, $T)$ and the lower one $\tau_{KWW}(Q = 2.93$ Å^{-1}, $T)$). The distribution of relaxation times for the β process is located between the dashed lines, which correspond to activation energies $E_0 + \sigma$ (upper one) and $E_0 - \sigma$ (lower one) (eq 9).

Thus, compared to PB the contribution of the secondary relaxation to the dynamic structure factor of PIB must be considerably weaker—nowhere in the experimental Q range does the β process does dominate $S(Q,t)$ but only induces shape changes. To visualize the temperature dependencies of the characteristic time scales involved, Figure 10 displays the dispersion zone of the Q-dependent relaxation times from Table 1 which all follow the shift factors $a_F(T)$ for the α relaxation. These times, as we will see, are characteristic for the α dispersion zone as could be observed in our experiment. The upper border corresponds to the largest times which are realized at $Q = 0.8$ Å^{-1}, while the lower border displays the shortest times measured at $Q = 2.93$ Å^{-1}. In addition Figure 10 displays the range of β-relaxation times taken from the dielectric results presented in Chapter IV.1. Here the upper and lower lines stand for the relaxation times corresponding to the distribution function $g(E)$ at $E = E_0 \pm \sigma$ (see eq 3b).

From the structure of $S^{\alpha\beta}(Q,t)$, where the α and β relaxation functions enter as a product (eq 7), it is immediately clear that the secondary process will only be visible if its time scale is at least equal or faster than that of the primary relaxation. Otherwise $S^{\alpha\beta}(Q,t)$ will have relaxed through $\varphi^{\alpha}(Q,t)$ before the relaxation of $S^{\beta}(Q,t)$ becomes significant. With this reasoning Figure 10 reveals that in particular at the lower temperatures we will have to expect an influence of the β-process on $S(Q,t)$. With the further observation that the β process does not dominate the spectra at any Q, we must conclude that its general contribution to $S(Q,t)$ is small.

Following eq 4 we therefore expect small values for the jump distances d.

We now turn to the quantitative evaluation of the spectra in terms of the dynamic structure factor discussed in section II: For the β process we assume a two-site jump process with a jump distribution and mean jump rate as found by dielectric spectroscopy (section IV.1). Fixing all parameters to those obtained from the dielectric experiment, the only variable connected to the β process then is the jump distance d.

For the relaxation function of the α process, we take a stretched exponential (eq 8) with a stretching parameter $\beta = 0.55$ corresponding to the line shape at the structure factor maximum. For the characteristic relaxation time $\tau_{KWW}(Q,t)$ a power law dependence on Q is assumed. Such a power law dependence is motivated from the Gaussian approximation

$$S(Q,t) \sim \exp\left[-\frac{Q^2\langle\Delta r^2(t)\rangle}{6}\right] = \exp\left\{-\left(\frac{t}{\tau_{KWW}(Q,T)}\right)^{\beta}\right\} \quad (12)$$

where $\langle\Delta r^2(t)\rangle$ is the mean squared atomic displacement. Equation 12 leads to $\tau_{KWW}(Q,t) = \tau^{\alpha}(T)\, Q^{-2/\beta}$.[31] Small deviations from the Gaussian behavior are taken into account by an exponent x/β where x is allowed to vary. For the temperature dependence of $\tau^{\alpha}(T)$ the rheological T law which has been shown to agree with the NSE data at the structure factor peak is taken. With these assumptions we fit the dynamic structure factor $S^{\alpha\beta}(Q,t)$ (eq 7) to the data.

Such a multiparameter nonlinear fit needs some care and a thoughtful approach. In a first evaluation the fit parameters were the jump distance d (eq 4), the power law exponent (x/β) in the Q dependence of $\tau_{KWW}(Q,t)$, and the prefactor τ_0^{α} for the α relaxation time. Furthermore the amplitudes $A(Q,t)$ of the different spectra were allowed to vary. With this approach all spectra at different Q and different temperatures were jointly fitted with eq 7. The fit leads to a good description of the spectra. As expected for the jump distance related to the β process a small value of $d = 0.5$ Å was extracted. For the power law exponent for the α relaxation times $x = 1.9$, very close to the Gaussian expectation of $x = 2$.

To scrutinize the multiparameter fit in some more detail, in a second approach, we tested for the momentum transfer dependence of $\tau_{KWW}(Q,t)$ in allowing a separate variation of the $\tau_{KWW}(Q,t)$ for each momentum transfer. Figure 11 displays the obtained Q-dependent times $\tau_{KWW}(Q,t)$ together with the result of the power law fit described above. We note that the independently evaluated $\tau_{KWW}(Q,t)$ scatter statistically around the power law determined above. In particular there is no evidence for a de Gennes' narrowing of the $\tau_{KWW}(Q,t)$, which would demand values for $\tau_{KWW}(Q,t)$ well above the power law in the peak region of $S(Q)$. For the jump distance d an individual variation of $\tau_{KWW}(Q,t)$ yields $d = 0.75$ Å.

Finally in order to test the assumption of identical prefactors for the β relaxation τ_0^{β} in the dielectric and the NSE experiment, we performed a fit floating also τ_0^{β} and allowing the $\tau_{KWW}(Q,t)$ to vary separately. This procedure results in a slightly larger value for τ_0^{β} ($\tau_0^{\beta} = 2.8 \times 10^{-13}$ s) and $d = 0.9$ Å. We note that for each of these fits the evaluated amplitudes $A(Q,t)$ for the different spectra displayed a systematic dependence on momentum transfer and temperature. In particular for each momentum transfer $\log[A(Q,t)]$ with good accuracy was found to depend linearly on temperature (see below).

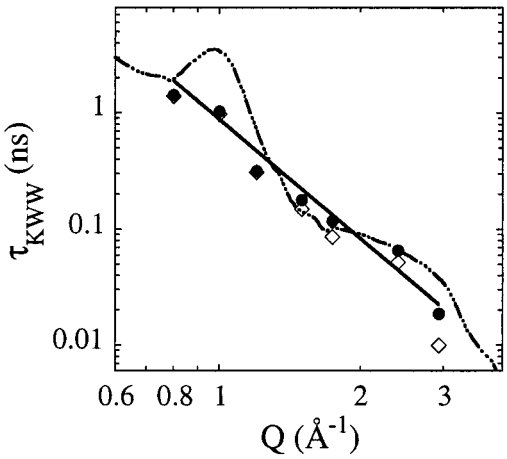

Figure 11. Q-dependence of the relaxation times $\tau_{KWW}(Q,t)$ for the α relaxation at 390 K: results of the fit of the NSE spectra to eq 7 (i) with a power law for $\tau_{KWW}(Q,t)$ (solid line) and (ii) allowing a separate variation for each Q (●). For comparison the times from Table 1 (fit of the NSE data to eq 8) are also shown (◇). The dashed-dotted line represents the prediction of the de Gennes' narrowing.

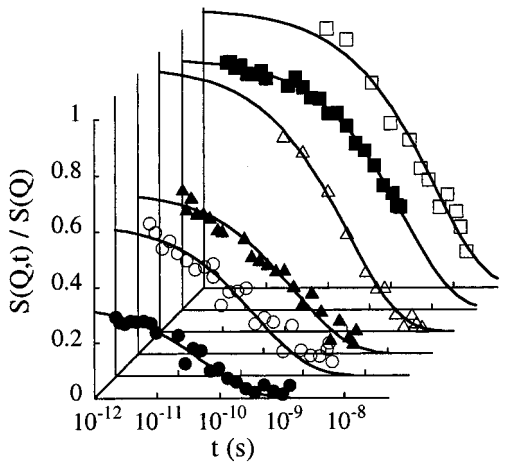

Figure 12. NSE spectra at 365 K and different Q-values: 0.8 Å^{-1} (□); 1.0 Å^{-1} (■); 1.2 Å^{-1} (△); 1.74 Å^{-1} (▲); 2.4 Å^{-1} (○); 2.93 Å^{-1} (●). Solid lines are the fit results (see text).

To demonstrate the quality of the data description in Figures 12 and 13 we show in an exemplary way the comparison of the fitted curves (second fit) and the data for the Q-dependent spectra at 365 K and for the temperature-dependent results for $Q = 1.74$ Å^{-1}. In each case very good agreement between the experimental results and the calculated dynamic structure factor is found. This agreement is practically identical for all three fitting approaches taken.

Following eq 5 Figure 14 displays the relative inelastic contribution (solid lines) to the dynamic structure factor for $d = 0.5$ Å and $d = 0.9$ Å together with $S(Q)$. As reasoned above due to the small value of the jump distance the β process only significantly contributes at higher Q values. In particular in the region of the first structure factor peak its contribution is very small not only at the peak itself but also at its flanks. This relates well to the phenomenological evaluation of section IV.2 (see Table 1), where a practically constant line shape in this peak region was found. In this respect the dynamic structure factor for PIB is qualitatively differ-

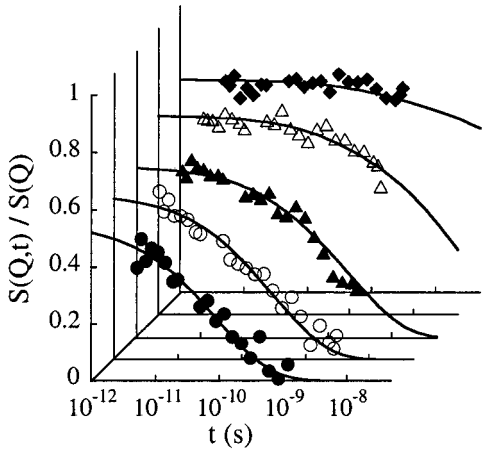

Figure 13. NSE spectra at 1.74 Å^{-1} and different temperatures: 270 K (◆); 300 K (△); 335 K (▲); 365 K (○); 390 K (●). Solid lines are the fit results (see text).

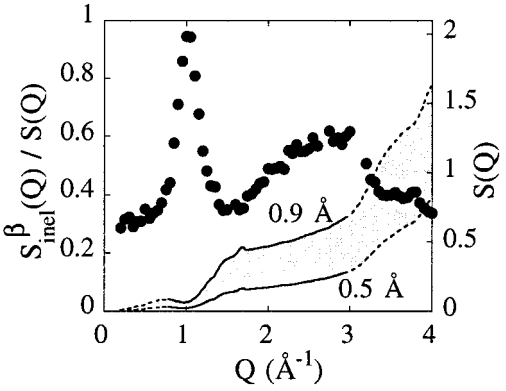

Figure 14. Q dependence of the relative quasielastic contribution from the β process to the coherent scattering function for jump distances of 0.5 and 0.9 Å (lines). The static structure factor $S(Q)$ is shown for comparison (●).

ent to that of PB, where at the wave vector of the structure factor minimum Q_{min} significant contributions of the β process were observed.

We now ask whether it is possible to relate the short jump distance found in the dynamic structure factor of PIB to some structural peculiarity of this polymer. Already the rotational isomeric state (RIS) calculations by Suter et al.[15] required a six state model, to describe the conformational characteristics properly. In this model each of torsional "trans" or "gauche" states is split into two substates giving rise to six different torsional states. Recently a Monte Carlo calculation by Vacatello and Yoon[16] confirmed this picture. The simulation revealed maps for the torsional potential displaying double minimum potentials split by about 15°. If transitions between these torsional minima occur, the largest motional jumps are carried out by the deuterium atoms in the methyl groups attached to the chain. Considering an isolated chain, a transition between the substates moves the scattering center of these methyl groups by about 1.1 Å. All other atoms move less. The distance of 1.1 Å is rather close to the values of $d \approx 0.5-0.9$ Å found from the evaluation of $S(Q,t)$, though beyond to what would be tolerated by the data. However, it is quite conceivable that in a dense bulk phase, where the adjacent chains impose resistance to motional excursion, the motional amplitudes of the methyl groups are reduced. Thus, we suggest that the secondary relaxation found in the dielectric experiments and identified with a jump length of $d \approx 0.5-0.9$ Å from the dynamic structure factor relates to these substate transitions.

Let us now turn to the α relaxation. We have already discussed in detail the temperature dependence (section IV.2), which follows very accurately the rheological α process. Here we concentrate on the dependence on momentum transfer. Three observations need some considerations: (i) the power law dependence over the entire Q-range investigated, (ii) the power law exponent $x = 1.9$ close to the Gaussian approximation of $x = 2$, and (iii) the virtual absence of a de Gennes' narrowing.

(i) For diffusive processes power law dependencies of the characteristic times are observed as long as the involved motional steps Δr are smaller than the spatial range $2\pi/Q$ probed by the scattering process.[32] In our experiment covering a Q range 0.8 Å$^{-1} \le Q \le 2.93$ Å^{-1} the observation of a power law covering the entire Q range thus means that the motion underlying the α process is rather continuous. The involved step widths Δr have to be smaller than about 1 or 2 Å.

(ii) The finding of a power law exponent very close to the Gaussian expectation first of all indicates a Gaussian distribution of mean squared displacements $\langle \Delta r^2(t) \rangle$ already in the angstrom regime which is appropriate for a diffusive process (see also Colmenero et al. in ref 31). We note that this observation is not trivial and point to the case of PB where strong deviations from such a Gaussian behavior were found.[19,33] Other than ordinary diffusion the mean squared displacements exhibit a sublinear time dependence, e.g., at 390 K (Table 1) those displacements become

$$\langle \Delta r^2(t) \rangle = 6.1[t\ (\mathrm{ns})]^{0.55}\ \text{Å}^2 \qquad (13)$$

Through the α process during 1 ns at 390 K on the average an atom of the PIB chain moves by about 2.5 Å. The sublinear time dependence of $\langle \Delta r^2(t) \rangle$ shows that the underlying diffusive pattern is not just a simple random walk but contains many unsuccessful diffusive attempts. The validity of the Gaussian approximation further indicates that the α relaxation at least within the temperature range investigated takes place in a spatially homogeneous rather than in a heterogeneous scenario.[34] Finally we emphasize that the time exponent close the value $^1/_2$ of the Rouse model should not be mistaken as due to Rouse dynamics.[35] The Q values of our experiment are far too large in order to fulfill the requirement of relaxing interconnected Gaussian segments being behind the Rouse model.

(iii) As for PB the Q dependence of the relaxation times $\tau_{KWW}(Q,t)$ involved in the α process do not exhibit the well-known de Gennes' narrowing which for simple liquids demands that the pair correlation function should display a modulation of the diffusive relaxation times $\tau = 1/D\,Q^2$ (D is the diffusion coefficient) with the structure factor $S(Q)$. To demonstrate the absence of such a narrowing in Figure 11 we have included the respective narrowing prediction $\tau_0^{\alpha}\,[Q^{-x}S(Q)]^{1/\beta}$ (dashed−dotted line). Obviously the experimental relaxation times disagree with this prediction. We remark that this discrepancy holds as well for the phenomenological times of Table 1 (see also Figure 11) and is not an artifact of the fitting procedure. While for PB a net narrowing of the spectra around Q_{max} occurs as a consequence of the suppression of the β process contributions (renormalization of the weights with $S(Q)$, see eq 5), for PIB these weights are minute around Q_{max} and even such a narrowing due to the secondary process

is absent. The obvious absence of any de Gennes' narrowing may indicate that the short range order giving rise to the peaks in $S(Q)$ (especially the interchain correlation at $Q = 1$ Å^{-1}) is only weakly affected by the motions involved in the α relaxation. Regions ΔV of a dimension implied by the width of the first structure factor peak, i.e., in the order of 15−20 Å may have to be considered as preferably moving together in the process of α relaxation. Thereby all parts of a region contribute with the same factor $\exp[-Q^2\langle r(t)^2\rangle]$ to the relaxation function.

Finally we comment on the amplitude factors $A(Q,T)$ determined in the fitting process of $S(Q,t)/S(Q)$ to the data. To interpret these quantities, we first have to understand what they are due to: As a result of the polarization analysis after the scattering process a NSE spectrometer offers only a limited band-pass to the scattered neutrons. Inelastically scattered neutrons with wavelengths λ shorter than the band-pass allows are not transmitted through the instrument and do not participate in the normalization of $S(Q,t)$ to $S(Q)$. Strictly speaking the $S(Q,t)$ values produced by the NSE spectrometer are not normalized to the full structure factor $S(Q) = \int_{-\infty}^{+\infty} S(Q,w)\mathrm{d}w$ but to a structure factor where the integral is taken only over the band-pass of the spectrometer.

The band of transmitted wavelengths depends on the analyzer setup of the instrument and on the neutron wavelength. Therefore the $A(Q,T)$ data taken at $\lambda = 7$ Å and $\lambda = 8$ Å cannot be compared with those at wavelengths essentially between 4 and 5 Å. For long wavelengths the band-pass is much narrower and accordingly the observed $A(Q,t)$ are higher than those at shorter wavelengths. Therefore, we concentrate on the short wavelength results.

At the used neutron wavelengths the IN11 band-pass allows for energy transfers up to about 2−3 meV. Thus the normalization of $S(Q,t)$ includes the so-called fast dynamical processes which are characteristic for glass-forming materials (fast relaxation processes,[30] Boson peak,[36] slow sound waves,[37] etc.) which for PIB are observed at energies below about 2 meV but excludes the ordinary vibrations. The amplitude parameters, therefore, should measure the decrease of $S(Q,t)$ due to these fast dynamical processes without being affected by the vibrational excitations above the band-pass.

In all cases the amplitudes $A(Q,t)$ may be described reasonably well by an apparent DWF for the fast dynamical processes

$$A(Q,T) = \exp\left[-\frac{Q^2\langle \Delta u_f^2(T)\rangle}{3}\right] \qquad (14)$$

where $\langle u_f^2(T)\rangle$ is the mean squared amplitude of those processes. A fit with eq 14 reveals the temperature dependence of $\langle u_f^2(T)\rangle$. Figure 15 presents the result. In the temperature range of observation $\langle u_f^2(T)\rangle$ follows a linear temperature dependence with an intersect at ≈160 K with the temperature axis. Figure 15 includes also mean square displacements $\langle u^2(T)\rangle$ from a measurement of the elastic Q-dependent intensity from a protonated PIB sample taken at the backscattering spectrometer IN16 of the ILL. These data correspond to those published recently by Frick and Richter[36] but provide better accuracy. As long as quasielastic broadening due to the α process does not take place, these mean squared displacements reflect the full DWF

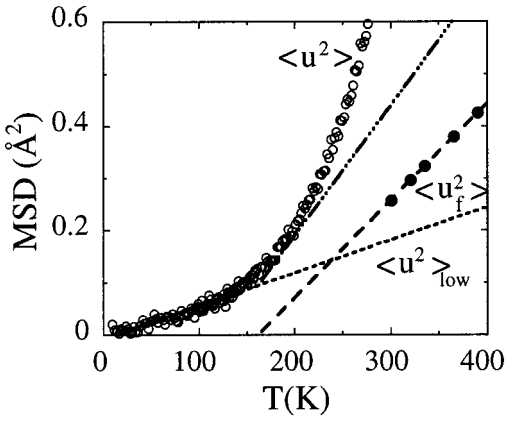

Figure 15. Temperature dependence of the mean squared displacements obtained from IN16 measurements $\langle u^2(T)\rangle$ (○) and from the fits of the NSE amplitudes to eq 14 $\langle u_f^2(T)\rangle$ (●). The dotted line shows the quasiharmonic extrapolation of the low-temperature mean squared displacements $\langle u^2(T)\rangle_{low}$; the dashed line corresponds to the linear regression fit of $\langle u^2(T)\rangle$. The addition of these two contributions is represented by the dashed-dotted line.

including all phonons. At low temperatures they exhibit a linear T dependence with considerably smaller slope than that for $\langle u_f^2(T)\rangle$ signifying a quasiharmonic phonon regime. Above about 140 K a strong upward turn of $\langle u^2(T)\rangle$ sets in reflecting the onset of the fast dynamical processes. At even higher temperature the broadening of the elastic line due to the α process further increases the now apparent $\langle u^2(T)\rangle$ values.

Considering that the low-temperature $\langle u^2(T)\rangle_{low}$ data reflect the complete phonon spectrum of PIB and that the phonons above energies of about 3−4 meV remain quasiharmonic (see Figure 6 in ref 36), we take the extrapolated low-temperature mean squared displacements as representative for the phonon-induced motions. The $\langle u_f^2(T)\rangle$ data obtained with the NSE spectrometer on the other hand exclude to a large extend the ordinary phonons and are characteristic for the amplitude of the fast dynamical processes. In a first approximation we may therefore add $\langle u_f^2(T)\rangle$ and $\langle u^2(T)\rangle_{low}$ in order to get an estimate for the total displacement. We note however that this approximation implies a double counting of those phonons within the band-pass of IN11—they contribute both to $\langle u_f^2(T)\rangle$ and to $\langle u^2(T)\rangle_{low}$. The result is displayed by a dashed−dotted line in Figure 15. It quantitatively agrees with the upturning mean squared displacement from the full DWF measurements. Only at higher temperatures when the α process itself causes first quasielastic broadening of the elastic line the then apparent $\langle u_f^2(T)\rangle$ increase above the dashed−dotted line. Thus, we find perfect agreement between the two quite different measurements taking place either in ω space or in the time regime underpinning the consistency of the procedures of the data evaluation undertaken. Furthermore combining NSE experiments and conventional DWF measurements allowed a nontrivial separation of phonon displacements and displacements due to the fast dynamical processes which we will explore in more detail in a future publication.

VI. Summary and Conclusions

We have presented a study on the molecular motions of polyisobutylene, where we have combined dielectric spectroscopy, a technique providing a very broad spec-

tral range, with high-resolution quasielastic neutron scattering offering space time resolution. Thereby dielectric spectroscopy informs about the breath of the dynamic processes and in particular about the distribution functions of relaxation times. With this knowledge as an input, neutron scattering then delivers unique insight into the space−time development of the molecular motions.

In a first phenomenological evaluation of the experimental results the following model independent results were achieved. (i) Aside from the primary relaxation the dielectric measurements revealed a secondary process distinctly different from the so far theoretically proposed γ and γ' relaxations. (ii) The neutron spin−echo spectra obtained at the Q value of the first structure factor peak, where the dynamic structure factor is selective to interchain motion, both agree with respect to the temperature dependence as well as to the shape with rheological results and disagree with spectroscopically based temperature laws. (iii) The Q-dependent spectra stretch with increasing Q while the characteristic relaxation times follow a power law dependence.

On the basis of a model dynamic structure factor which incorporates primary and secondary relaxations under the assumption of their mutual statistical independence and simultaneous occurrence, we have quantitatively evaluated the momentum transfer and temperature-dependent spectra. Thereby knowledge on the distribution parameters and the temperature dependence for the β process was taken as an input from the dielectric experiments. With this dynamic structure factor a very good data description could be achieved. The following results pertain: (i) The jump distance involved in the β process amounts to only $d = 0.5-0.9$ Å being significantly smaller than the corresponding value of $d = 1.5$ Å found for PB. The extracted distance relates well to molecular displacements expected for substate transitions in the double minimum potential for the split conformational states of PIB. (ii) The α-relaxation times $\tau_{KWW}(Q,t)$ follow a power law in Q with an exponent close to the expectation from the Gaussian approximation. (iii) The extent of this power law in Q limits the step width connected with the diffusive α process to less than 2 Å. (iv) Though studying the pair correlation function, where at least for simple liquids a de Gennes' narrowing of the diffusive relaxation rates would be expected, the Q-dependent α-relaxation times do not exhibit any significant modulation with $S(Q)$. (v) The determined spectral amplitudes reveal the mean squared displacements associated with the fast dynamical processes. The obtained values are in very good agreement with conventional DWF measurements on a protonated PIB sample using a high-resolution backscattering spectrometer.

We conclude that exploiting the complementarity of broad band spectral methods such as dielectric spectroscopy and high-resolution neutron scattering has the potential to reveal deeper insight into the molecular motions in polymeric systems which could not be achieved applying only one of the techniques. We also would like to express our hope that this study may stimulate investigations by computer simulation which together with the experiment could lead to an even deeper level of understanding of these molecular processes.

Acknowledgment. We acknowledge partial support by the Acciones Integradas Spain-Germany (Contract: AI 95-09). Financial support from the Spanish CICyT, project MEC PB94-0468, is acknowledged by J. Colmenero; A. Arbe also acknowledges the Grant of the Basque Government. We are thankful to Professor A. Alegría, Dr. H. Grimm, and A. Wischnewski for experimental help.

References and Notes

(1) Ferry, J. D. In *Viscoelastic Properties of Polymers*; John Wiley & Sons: New York, 1970.
(2) Fitzgerald, E. R.; Grandine, L. D., Jr.; Ferry, J. D. *J. Appl. Phys.* **1953**, *24*, 650. Ferry, J. D.; Grandine, L. D., Jr.; Fitzgerald, E. R. *J. Appl. Phys.* **1953**, *24*, 911.
(3) Philippoff, W. *J. Appl. Phys.* **1953**, *24*, 685.
(4) Tobolsky, A. V.; Catsiff, E. *J. Polym. Sci.* **1956**, *19*, 111.
(5) Plazek, D. J.; Vranken, M. N.; Berge, J. W. *Trans. Soc. Rheol.* **1958**, *2*, 39.
(6) Törmälä, P. *J. Macromol. Sci.-Rev. Macromol. Chem. C* **1979**, *17*, 297.
(7) Plazek, D. J.; Zheng, X. D.; Ngai, K. L. *Macromolecules* **1992**, *25*, 4920.
(8) Ngai, K. L.; Plazek, D. J.; Bero, C. A. *Macromolecules* **1993**, *26*, 1065.
(9) Plazek, D. J.; Chay, I.-C.; Ngai, K. L.; Roland, C. M. *Macromolecules* **1995**, *28*, 6432.
(10) Angell, C. A.; Monnerie, L.; Torell, L. M. In *Structure, Relaxation, and Physical Aging of Glassy Polymers*; Roe, R. J., O'Reilly, J. M., Eds.; Materials Research Society Symposium Proceedings; Materials Research Society: Pittsburgh, PA, 1991; Vol. 215, p 3.
(11) Slichter, W. P. *J. Polym. Sci.: Part C* **1966**, *14*, 33.
(12) Dejean de la Batie, R.; Lauprêtre, F.; Monnerie. L. *Macromolecules* **1989**, *22*, 2617.
(13) McCrum, N. G.; Read, B. E.; Williams, G. In *Anelastic and Dielectric Effects in Polymeric Solids*; Wiley: London, 1967; p 389.
(14) Stoll, B.; Pechhold, W.; Blasenbrey, S. *Kolloid-Z.* **1972**, *250*, 1111.
(15) Suter, U. W.; Saiz, E.; Flory, P. J. *Macromolecules* **1983**, *16*, 1317 and references therein.
(16) Vacatello, M.; Yoon, D. Y. *Macromolecules* **1992**, *25*, 2502.
(17) Hayashi, H.; Flory, P. J. Wignall, G. D. *Macromolecules* **1983**, *16*, 1328.
(18) Arbe, A.; Buchenau, U.; Willner, L.; Richter, D.; Farago, B.; Colmenero, J. *Phys. Rev. Lett.* **1996**, *76*, 1872.
(19) Arbe, A.; Richter, D.; Colmenero, J.; Farago, B. *Phys. Rev. E.* **1996**, *54*, 3853.
(20) See, e.g.: *Neutron Spin-Echo*; Mezei, F., Ed.; Lecture Notes in Physics; Springer-Verlag: Heidelberg, 1980; Vol. 28.
(21) See, e.g.: Bee, M. In *Quasielastic Neutron Scattering*; Adam Hilger: Bristol, 1988.
(22) Johari, G. P.; Goldstein, M. *J. Chem. Phys.* **1970**, *53*, 2372.
(23) de Gennes, P. G. *Physica* **1959**, *25*, 825.
(24) Györ, M.; Fodor, Zs.; Wang, H.-C.; Faust, R. *J. Macromol. Sci.−Pure Appl. Chem.* **1994**, *A31*, 2053.
(25) For experimental details, see, e.g.: Hofmann, A.; Alegría, A.; Colmenero, J.; Willner, L.; Buscaglia, E.; Hadjchristidis, N. *Macromolecules* **1996**, *29*, 129.
(26) Monkenbusch, M.; Schätzler, R.; Richter, D. *Nuclear Instruments and Methods* **1997**, *A399*, 301.
(27) Williams, G. *Adv. Polym. Sci.* **1979**, *33*, 60.
(28) Farago, B. *ILL Annu. Rep.* **1988**, 103.
(29) Frick, B.; Richter, D. *Science* **1995**, *167*, 1939.
(30) Colmenero, J.; Arbe, A.; Alegría, A. *Phys. Rev. Lett.* **1993**, *71*, 2603.
(31) Colmenero, J.; Alegría, A.; Arbe, A.; Frick, B. *Phys. Rev. Lett.* **1992**, *69*, 478.
(32) See, e.g.: Springer, T. In *Quasielastic Neutron Scattering for the Investigation of Diffusive Motions in Solids and Liquids*; Springer Tracts in Modern Physics; Springer: Berlin, 1972.
(33) Zorn, R.; Arbe, A.; Colmenero, J.; Frick, B.; Richter, D.; Buchenau, U. *Phys. Rev. E* **1995**, *52*, 781.
(34) Cicerone, M. T.; Ediger, M. D. *J. Chem. Phys.* **1996**, *104*, 7210.
(35) Allen, G.; Higgins, J. S.; Macounachie, A.; Ghosh, R. E. *Chem. Soc. Faraday Trans. 2* **1982**, *78*, 2117.
(36) Frick, B.; Richter, D. *Phys. Rev. B* **1993**, *47*, 14795.
(37) Buchenau, U.; Wischnewski, A.; Richter, D.; Frick, B. *Phys. Rev. Lett.* **1996**, *77*, 4035.

MA971340G